Optical waveguide intensity modulators based on a tunable electron density multiple quantum well structure

J. E. Zucker, M. Wegener, K. L. Jones, T. Y. Chang, N. Sauer, and D. S. Chemla

Citation: Applied Physics Letters **56**, 1951 (1990); doi: 10.1063/1.103032
View online: http://dx.doi.org/10.1063/1.103032
View Table of Contents: http://scitation.aip.org/content/aip/journal/apl/56/20?ver=pdfcov
Published by the AIP Publishing

Optical waveguide intensity modulators based on a tunable electron density multiple quantum well structure

J. E. Zucker, M. Wegener, K. L. Jones, T. Y. Chang, N. Sauer, and D. S. Chemla
AT&T Bell Laboratories, Holmdel, New Jersey 07733

(Received 8 January 1990; accepted for publication 5 March 1990)

With a recently developed semiconductor heterostructure it has become possible to tune continuously the electron density in multiple quantum wells. Here we demonstrate the first electro-optic waveguide intensity modulators based on this concept. We achieve a 22 dB ON/OFF ratio for 9 V applied at 1.54 μm wavelength in a rib waveguide electroabsorption modulator. Electrorefractive devices include a waveguide Mach–Zehnder interferometer with an active length 650 μm operating at 1.58 μm wavelength with 5.4 V half-wave voltage. We show that the operating voltage can be further reduced by operating the Mach–Zehnder modulators in push-pull configuration.

The trend toward higher bit rates in optical communications systems has prompted a search for external intensity modulators in order to avoid the frequency chirping of directly modulated lasers.[1] In this letter we demonstrate how electroabsorption (EA) and electrorefraction (ER) in a novel quantum mechanically engineered heterostructure can be applied to waveguide intensity modulators in the 1.55 μm wavelength range. We employ the barrier reservoir and quantum well electron transfer structure (BRAQWETS)[2] in two distinct waveguide architectures: an in-line rib waveguide EA modulator operating at 1.54 μm wavelength and a Mach–Zehnder ER interferometer that operates at longer wavelengths 20–30 meV below the band edge. These prototype components illustrate the strengths of the BRAQWETS band filling effect for extremely compact, low-voltage waveguide device applications.

Each BRAQWETS fundamental period independently provides large voltage-induced changes in oscillator strength by controlled electron transfer into a quantum well (QW).[2] In the present waveguide structure, five fundamental periods, each containing one 90 Å InGaAs QW, are stacked to form the 0.76-μm-thick core. The top and bottom Si-doped InAlAs cladding layers are 3200 and 900 Å thick, respectively. Figure 1(a) shows the calculated intensity distribution for the fundamental mode of the unetched wafer, with the upper cladding, the lower cladding, and 5300 Å of the n^+-InP substrate appearing as shaded regions. The five QWs in the unshaded core are shown to scale. For this structure, we calculate that the waveguide confinement factors Γ_{QW} for each QW range from 7.6×10^{-3} to 1.3×10^{-2} depending on proximity to the mode center; the sum for all five is $\Gamma_{TOT} = 5.0\times10^{-2}$.

Rib waveguide devices are formed by wet chemical etching with 1:1:38 H_3PO_4:H_2O_2:H_2O through the top cladding, the core, and 300 Å of the lower cladding. The total etch depth of 1.05 μm provides good electrical isolation (>120 MΩ) between ribs as well as good lateral optical confinement. The EA modulator, shown schematically in Fig. 1(b), has rib width $w = 10$ μm and length $L = 1.04$ mm. The Mach–Zehnder interferometers, shown in Fig. 1(c), have rib width $d = 5$ μm, and active lengths L ranging from 350 to 650 μm. The active sections are isolated from the Y-branch by 3-μm-wide, 1.05-μm-deep etched grooves. Voltage V is applied between the top of the rib and the grounded substrate. Electrical pads for both structures are 60 μm $\times$ 60 μm. For voltages between -4 and $+5$ V, the leakage current I is <10 μA. To avoid undesirable current-induced effects such as heating, we have been careful to keep voltages within the range $V = +7$ V, where $I = +50$ μA and $V = -5$ V, where $I = -30$ μA. The transmission charac-

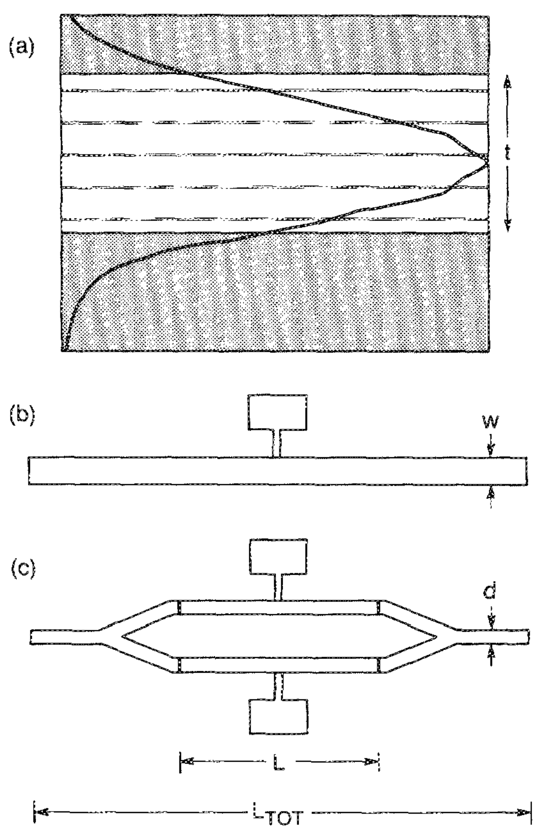

FIG. 1. (a) Side view of unetched wafer structure and calculated mode intensity profile, drawn to scale. Thickness of core region $t = 0.76$ μm, lines within show the five quantum wells. (b) Top view schematic of rib waveguide in-line intensity modulator, $w = 10$ μm. (c) Top view of Mach–Zehnder interferometric intensity modulators: $d = 5$ μm, $L = 350$, 450, 550, 650 μm, $L_{TOT} = 770$, 840, 1000, 1250 μm.

teristics as a function of voltage are determined by coupling TE-polarized light from InGaAsP laser diodes or a cw yittrium lithium fluoride (YLF:Nd)-pumped NaCl-F^{2+} color center laser into and out of the devices by means of microscope objectives. The near-field output intensity is observed with an infrared TV camera and measured with Ge or PbS detectors.

Figure 3 shows the ON/OFF ratio at 1.54 μm wavelength for the EA modulator as a function of voltage. The OFF state is defined as the transmission at $V_0 = -2$ V, where maximum attenuation of the output is achieved. This high absorption state is characteristic of a quantum well that contains no electrons. As voltage is increased, electrons are efficiently transferred into each well from an individual reservoir, bleaching the QW excitonic absorption. Thus the waveguide output intensity continues to increase with applied voltage. Two distinct voltage regimes are apparent in Fig. 2: for $V_0 < V < 0$ V the ON/OFF ratio per volt is 5.5 times smaller than that for $V > 0$. We interpret the low-voltage behavior in terms of EA associated with a reverse quantum-confined Stark effect (QCSE).[2,3] The applied field opposes the built-in field of the structure. Therefore with increasing voltage we decrease the field across the QW, reversing the red shift of the QCSE. For the voltage swing $V_0 \to 0$, the net decrease in the absorption coefficient of the waveguide is $\Delta\alpha = 21.1\ \mathrm{cm}^{-1}$. On the other hand for $V > 0$, the increased transmission reflects phase space absorption quenching (PAQ) by free electrons.[4] For the voltage swing $0 \to 7$ V, $\Delta\alpha = 27.5\ \mathrm{cm}^{-1}$. When scaled up by the waveguide confinement factor Γ_{TOT}, $\Delta\alpha/\Gamma_{\mathrm{TOT}}$ is in reasonable agreement with $\Delta\alpha$ measured in the BRAQWETS at normal incidence.[5] For the entire 9 V voltage swing ($-2 \to +7$ V), which corresponds to 1.8 V applied across each QW, we achieve modulation depth larger than 20 dB at 1.54 μm wavelength. The propagation loss of the 1.04-mm-long modulator in the ON state, i.e., $+7$ V applied, is 3 dB at 1.54 μm.

We have also measured the propagation loss of 5-μm-wide straight rib guides at zero bias at wavelengths between 1.54 and 1.60 μm using the cutback method. We find an exponential dependence of the waveguide absorption on $\Delta\omega$, the energy detuning from the ground state exciton resonance: $\alpha = \alpha_0 e^{-\Delta\omega/E_0}$ with $E_0 = 19.6$ meV and $\alpha_0 = 34.5\ \mathrm{cm}^{-1}$. Thus at 1.6 μm the propagation loss at zero bias is 2.5 dB/mm. A large component of the propagation loss in the present BRAQWETS waveguide is due to scattering of the mode by interface roughness since there is a large index discontinuity between the rib and air. Nevertheless, we achieve lower propagation loss here than in *p-i-n* strip-loaded QW waveguides with comparable lateral dimension. This suggests that the absence of undepleted *p*-doped layers in the BRAQWETS waveguide is a significant advantage in terms of lowered waveguide loss.

The absorption blue shift in the BRAQWETS allows optical phase modulation with minimal intensity modulation at wavelengths below the band edge.[5] Hence BRAQWET ER devices can operate at smaller detunings from the exciton resonance than red-shifting devices based on the QCSE. This is illustrated in Fig. 3(a), where we show the modulation characteristic of a Mach–Zehnder waveguide interferometer at wavelength 1.58 μm, only 26 meV detuned from the ground-state exciton absorption peak. The output intensity as a function of bias remains sinusoidal and undamped even at the highest voltage, showing that EA at this wavelength is negligible.[6] This observation is in agreement with the ratio of phase-to-intensity modulation found in normal incidence propagation through the BRAQWETS[5] $\Delta n/\Delta k \sim 10$, ten times larger than the corresponding figure for the QCSE.

Figure 3(a) shows that for a Mach–Zehnder modulator with $L = 650$ μm the voltage needed to achieve 180° phase shift V_π is 5.4 V at 1.58 μm. Good agreement between the data (circles) and a constant frequency raised cosine (solid line) shows that Δn is linear in the applied voltage,[2,5] with

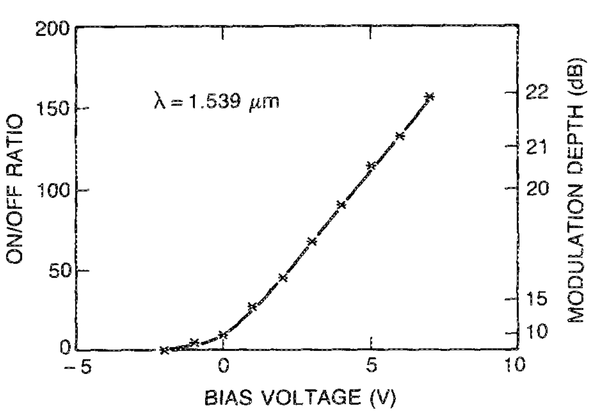

FIG. 2. ON/OFF ratio as a function of applied bias for rib waveguide electroabsorption modulator at 1.539 μm wavelength, TE polarization. OFF state is with -2 V applied.

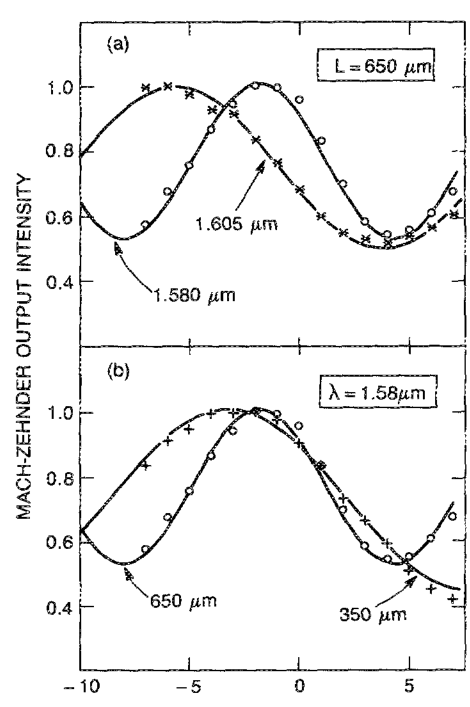

FIG. 3. Mach–Zehnder output intensity as a function of single arm drive voltage (a) for 650-μm-long active length device at wavelengths 1.58 μm (circles) and 1.605 μm (stars) and (b) at 1.58 μm for two different active lengths 650 μm (circles) and 350 μm (crosses).

the fit yielding the waveguide effective index change per volt $\Delta n/V = 2.2\times10^{-4}$ V^{-1} at 1.58 μm. At a fixed voltage, Δn falls off with increasing detuning from the band edge. Thus the voltage required V_π will increase with wavelength. At 1.605 μm, Fig. 3(a) shows $V_\pi = 9.5$ V for $L = 650\,\mu$m, with $\Delta n/V = 1.3\times10^{-4}$ V^{-1}.

With a linear electro-optic effect, i.e., $\Delta n \propto V$, there is a direct tradeoff between device voltage and length. At a given wavelength, the product $V_\pi \times L$ should remain constant. This is shown in Fig. 3(b), where we compare the output characteristics at 1.58 μm for $L = 350\,\mu$m and $L = 650\,\mu$m. For the $L = 350\,\mu$m device, $V_\pi = 11.8$ V, 15% higher than the value that would be expected from the ratio of the lengths.

It is interesting to gauge the performance of the BRAQWET Mach–Zehnder against more mature material systems. The best value for the voltage-length product needed to switch a $LiNbO_3$ interferometric modulator at 1.58 μm wavelength is 4.7 V-cm.[7] Recently a bulk InGaAsP/InP waveguide interferometric modulator at 1.55 μm was reported with $V_\pi \times L = 2.25$ V-cm.[8] The corresponding figure of merit for the $L = 650\,\mu$m BRAQWETS device at 1.58 μm is $V_\pi \times L = 0.35$ V-cm. The prospects for further reduction in $V_\pi \times L$ are good, since the current BRAQWETS period contains a 500 Å InGaAlAs electron reservoir layer and a 600 Å InAlAs barrier layer. By decreasing these thicknesses, we expect to achieve a waveguide with higher Γ_{TOT} and thus higher voltage sensitivity.

The Mach–Zehnder interferometric modulator architecture has the advantage that it provides intensity modulation with zero phase modulation as long as both arms experience equal and opposite Δn.[1] In addition, when both arms of the modulator are used in push-pull configuration, the half-wave voltage can be significantly reduced. This is demonstrated in Fig. 4, where an ac switching voltage of the same magnitude but opposite phase is applied to the two arms of an $L = 550\,\mu$m device in addition to some dc prebias. The voltage required for complete modulation in push pull configuration (dashed line) is only $V_\pi^{pp} = 4$ V, half that shown for single arm drive (solid line).

In conclusion, we have demonstrated the first application of the BRAQWETS concept to waveguide intensity modulators and have investigated both electrorefractive and electroabsorptive devices. In high-speed or high optical power applications, the ER BRAQWETS modulator may be preferred over the EA modulator. For the EA modulator presented here, we have $\Delta n/\Delta k = 4$ at 1.539 μm. This will cause a frequency chirp which is about the same as that obtained by directly modulating a conventional laser diode.[1] On the other hand, the optical response of the ER device operating far below the band edge will not saturate with high optical intensity and, as discussed above, the frequency chirp under high-speed operation can be minimized in an interferometric modulator in push-pull configuration. Although the electron-induced optical changes in the BRAQWETS are just as large as band filling effects in carrier injection devices, the response times are not limited by electron-hole recombination. The fundamental switch-on and switch-off time of BRAQWET-based modulators is determined by the transit time of electrons across the spacer between the reservoir and QW. Pump-probe optical measurements indicate that this process takes <20 ps at zero bias. Practically the electro-optic modulation bandwidth will be determined by the device RC time; we measure that the capacitance of one arm of an $L = 350\,\mu$m Mach–Zehnder is 1.95 pF including the pad. Assuming 50 Ω drive, this implies operation above 1 GHz, well beyond the 50 MHz limit imposed by recombination times in carrier injection devices.

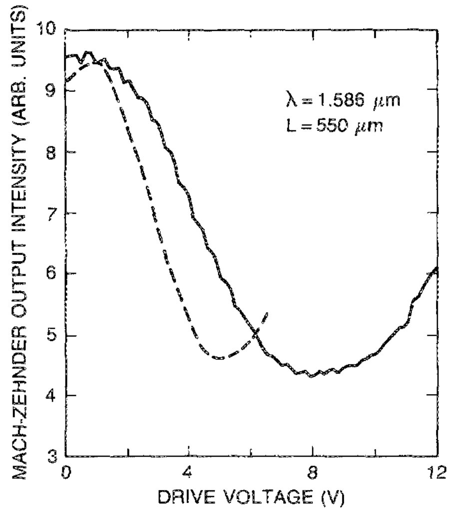

FIG. 4. Mach–Zehnder output intensity of a 550-μm-long active length device at 1.586 μm. Solid line, single arm drive with dc prebias $V1 = -4$ V, $V2 = -2$ V; dashed line, dual arm drive in push-pull operation with dc prebias $V1 = -4$, $V2 = -1$ V.

[1]F. Koyama and K. Iga, J. Lightwave Technol. **6**, 87 (1988).
[2]M. Wegener, T. Y. Chang, I. Bar-Joseph, J. M. Kuo, and D. S. Chemla, Appl. Phys. Lett. **55**, 583 (1989); M. Wegener, J. E. Zucker, T. Y. Chang, N. J. Sauer, K. L. Jones, and D. S. Chemla, Phys. Rev. B **41**, 3097 (1990).
[3]D. A. B. Miller, D. S. Chemla, T. C. Damen, A. C. Gossard, W. Wiegmann, T. H. Wood, and C. A. Burrus, Phys. Rev. B **32**, 1043 (1985).
[4]D. S. Chemla, I. Bar-Joseph, C. Klingshirn, D. A. B. Miller, J. M. Kuo, and T. Y. Chang, Appl. Phys. Lett. **50**, 585 (1987).
[5]J. E. Zucker, T. Y. Chang, M. Wegener, N. J. Sauer, K. L. Jones, and D. S. Chemla, Photonics Technol. Lett. **2**, 29 (1990).
[6]R. A. Soref, D. L. Mc Daniel, and B. R. Bennett, J. Lightwave Technol. **6**, 437 (1988).
[7]S. K. Korotky and R. C. Alferness, in *Optical Fiber Telecommunications*, edited by I. P. Kaminow and S. E. Miller (Academic, New York, 1988), pp. 421–465.
[8]H. Takeuchi, K. Kasaya, and K. Oe, IEEE Photonics Technol. Lett. **1**, 227 (1989).